Human fucosyltransferase 6 enables prostate cancer metastasis to bone

FULL PAPER

BJC

British Journal of Cancer (2013) 109, 3014–3022 | doi: 10.1038/bjc.2013.690

Keywords: fucosyltransferase; prostate cancer; E-selectin; homing; bone metastasis

Human fucosyltransferase 6 enables prostate cancer metastasis to bone

J Li[1], A D Guillebon[1], J-w Hsu[1], S R Barthel[2,3], C J Dimitroff[2,3], Y-F Lee[4] and M R King[*,1]

[1]Department of Biomedical Engineering, Cornell University, Ithaca, NY 14853, USA; [2]Department of Dermatology, Brigham and Women's Hospital, Boston, MA 02115, USA; [3]Harvard Medical School, Boston, MA 02115, USA and [4]Department of Urology and Pathology Laboratory Medicine, University of Rochester Medical Center, Rochester, NY 14642, USA

Background: The interaction between human prostate cancer (PCa) cells and bone marrow (BM) endothelium follows a rolling-and-adhesion cascade mediated by E-selectin ligand (ESL): E-selectin. This adhesion is enabled by elevated expression of α-1, 3-fucosyltransferases (FTs), enzymes responsible for ESL-mediated bone metastasis in humans. In contrast, the incidence of bone metastasis in mice is rare.

Methods: FT 3, 6 and 7 were overexpressed in mouse PCa cells. The rolling cell number, cell-rolling velocity and transendothelial migration were characterised *in vitro*. Fucosyltransferases-transduced mouse PCa cells expressing luciferase were inoculated into mice via left ventricle to compare the capability of bone metastasis. Mass spectrometry and immunoprecipitation were utilised for identification of ESLs.

Results: Overexpression of FT3, FT6 or FT7 restored ESLs and enabled mouse PCa cells to roll and adhere in E-selectin-functionalised microtubes, similar to trafficking of circulating PCa cells in BM vessels. Following intracardiac inoculation, FT6-transduced cells induced robust bone metastasis in mice. Inhibition of FT6 by a fucose mimetic significantly reduced bone metastasis. Importantly, comparison of FT3, FT6 and FT7 gene expression in existing clinical samples showed significant upregulation of FT6 in PCa-distant metastases.

Conclusion: FT6 is a key mediator of PCa cells trafficking to the BM. It may serve as a viable drug target in preclinical tests of therapeutics for reduction of PCa bone metastasis.

Prostate cancer (PCa) is the leading cause of cancer death among American men, second only to lung cancer in 2012. When detected at an early stage, the 5-year survival rate is close to 100%. In contrast, if diagnosed at a late stage with advanced metastatic disease, the 5-year survival decreases to 33% (Siegel *et al*, 2012). The most common metastatic sites of PCa are lymph nodes, bones, lung and liver (Wilt and Ahmed, 2013). Among these sites, bone is the most challenging organ for therapeutic intervention as bone metastasis can cause severe skeleton-related diseases such as bone pain, hypercalcemia, fractures and nerve compression syndromes (Saad *et al*, 2006; Sturge *et al*, 2011).

Metastasis to bone is a multistep cascade. Prostate cancer cells detached from the primary site must first invade a blood vessel, a process called intravasation. Through hematogenous dissemination, a sub-population of cells attach to bone marrow (BM) endothelial cells. This process is mediated by multiple receptor–ligand interactions under shear stress, referred to as a rolling-and-adhesion cascade (Li and King, 2012). This cascade further facilitates PCa cells to breach the bone endothelial layer (transendothelial migration; TEM) to establish micrometastases in the bone microenvironment (Barthel *et al*, 2013).

Bone marrow endothelial cells constitutively express E-selectin, which enables homing of hematopoietic stem cells expressing E-selectin ligands (ESLs) to the BM (Sackstein, 2012; Winkler *et al*, 2012). Recent studies have indicated that human PCa cells also express similar ESLs to interact and traverse the vasculature of the BM (Dimitroff *et al*, 2004, 2005; Barthel *et al*, 2013). E-selectin ligands comprise the tetrasaccharide sialyl Lewis X (sLe^x) attached

*Correspondence: Professor MR King; E-mail: mike.king@cornell.edu

Revised 8 October 2013; accepted 9 October 2013;
published online 31 October 2013

to the extracellular domain of glycoproteins or glycolipids. The synthesis of sLe^x on such glycoproteins is catalysed in the Golgi compartment by members of the glycosyltransferase gene family. The final step involves the transfer of fucose to *N*-acetylglucosamine at the terminal α-2, 3 sialo-lactosamine unit by α-1, 3-fucosyltransferases (FT) 3, 4, 5, 6 and/or 7 depending on the cell type (de Vries *et al*, 2001). Gene expression profiling and immunohistology in several human PCa cell lines have shown that the bone metastasis potential correlates well with the expression level of FTs (Barthel *et al*, 2008; Yin *et al,* 2010). To the contrary, the rare evidence of bone metastasis in mice genetically prone to PCa raises the question of whether mouse PCa cells express ESLs (Gingrich *et al*, 1996). Moreover, if they are absent in mouse PCa cells, can one develop a new mouse model with robust bone metastasis by increasing expression of functional ESLs?

MATERIALS AND METHODS

Cell lines and mice. The transgenic adenocarcinoma of the mouse prostate (TRAMP) cell lines TRAMP-C1 and TRAMP-C2 were obtained from American Type Culture Collection (ATCC; Rockville, MD, USA) and cultured in Dulbecco's modified Eagle's medium (Invitrogen, Grand Island, NY, USA) with 4 mM L-glutamine adjusted to contain 1.5 g l^{-1} sodium bicarbonate and 4.5 g l^{-1} glucose supplemented with 0.005 mg ml^{-1} bovine insulin and 10 nM dehydroisoandrosterone, 90%; fetal bovine serum (BD Biosciences, San Jose, CA, USA), 5%; Nu-Serum IV (BD Biosciences), 5%. RM1 cells are a murine- androgen-insensitive PCa cell line, which were kindly provided by T Thompson (MD Anderson Cancer Center, Houston, TX, USA) for this study. RM1 cells were cultured in Dulbecco's modified Eagle's medium supplemented with 10% FBS. Human umbilical vein endothelial cells (HUVEC) were obtained from ATCC and cultured in vascular cell basal medium (ATCC) using the endothelial cell growth kit-BBE (ATCC PCS-100-040). Human umbilical vein endothelial cells were used up to passage number 6. Six- to 8-week-old male C57BL/6 mice were purchased from Jackson Laboratory (Bar Harbor, ME, USA). Mice were housed in a SPF barrier animal facility at the Cornell University.

Antibodies. The following recombinant proteins or antibodies were employed to characterise ESLs in this study: recombinant mouse E-selectin/CD62E Fc chimera (R&D Systems, Minneapolis, MN, USA), PE goat anti-human IgG (Santa Cruz Biotech, Santa Cruz, CA, USA), FITC HECA-452 (BD Biosciences), PE anti-mouse PSGL-1 (BD Biosciences) and FITC anti-mouse CD44 (BD Biosciences). The following antibodies from BD Biosciences were used as isotype controls: FITC Rat IgG2b, FITC Rat IgM and PE Rat IgG1.

Flow cytometry. Cells were detached with enzyme-free Gibco Cell Dissociation Buffer (Invitrogen) and suspended at a concentration of 5×10^5 cells in 100 μl cold PBS/1% bovine serum albumin (BSA). Primary antibodies or corresponding isotype control antibodies were incubated with cells for 30 min on ice. Following two washes with 1 ml PBS/1% BSA, fluorescence measurements were collected on an Accuri C6 flow cytometer (BD Biosciences). Data were analysed using the Flow Express software (*De Novo* Software, Los Angeles, CA, USA). Cells were gated based on forward and side scatter. For detection of ESLs, recombinant mouse E-selectin/CD62E Fc chimera was used at a concentration of 10 μg ml^{-1}. Cells were suspended at a concentration of 5×10^5 cells in 100 μl cold binding buffer PBS/1% BSA/2 mM Ca^{2+} or control buffer PBS/1% BSA/1 mM EDTA. Incubation was performed for 30 min on ice. Cells were washed with binding buffer or control buffer twice and stained with secondary PE anti-human IgG for 30 min on ice.

Western blotting and immunoprecipitation. For western blotting, whole-cell lysates were prepared and separated by 8% SDS–PAGE as previously described (Bu *et al,* 2013). Membranes were incubated with primary antibodies HECA-452 (BD Biosciences), anti-β actin (Santa Cruz Biotech) and recombinant mouse E-selectin-Fc (R&D Systems). All primary antibodies were diluted 1 : 1000. Mouse E-selectin-Fc was diluted to 1 μg ml^{-1} in the presence of 2.5 mM $CaCl_2$. Immunoprecipitation was performed to identify E-selectin-reactive membrane protein as previously described (Matsumoto *et al*, 2005). Five hundred micrograms of precleared proteins were incubated with either 5 μg human IgG isotype or 5 μg mouse E-selectin-Fc. The prepared samples were separated and analysed by western blotting. Anti-CD44 (Biolegend, San Diego, CA, USA) was used at 1 : 1000 dilution in the blotting.

Identification of E-selectin-Fc-reactive protein by mass spectrometry. Lysates from empty vector- and FT6-transduced TRAMP-C2 were subjected to immunoprecipitation by E-selectin-Fc. Proteins that interacted with E-selectin-Fc were analysed by 8% SDS–PAGE. To guide localisation, excision and retention of the relevant protein, an E-selectin-Fc-immunostained blot was prepared from the same gel. The stained blot was superimposed with the corresponding gel to excise the fragment in the gel. The fragment was digested with trypsin and analysed by nano HPLC MS/MS with Orbitrap Elite (Thermo Fisher Scientific Inc., Waltham, MA, USA), and the NCBI database was searched for possible peptide matches. The peptide sequences from empty vector-transduced samples were used as background control to exclude non-specific interaction with E-selectin-Fc.

Retroviral production and transduction. Retroviral vectors encoding human α-1,3 FT3, FT6, FT7 and retrovirus packaging helper plasmids pN8e-gag_pol_deltaS and pN8e-VSV-G were utilised. Briefly, retroviral vectors and two helper plasmids were transfected into HEK293T cells by TransIT-LT1 Transfection Reagent (Mirus Biology, Madison, WI, USA). Virus supernatants were collected at 48 and 72 h after transfection. Virus supernatants were mixed with target cells in the presence of 8 μg ml^{-1} polybrene (Santa Cruz Biotech) for 24 h. Afterwards, fresh media was added and cells were selected with 200 μg ml^{-1} G418 for 2 weeks.

Tumour cell TEM assay. The QCM Tumor Cell Transendothelial Migration Assay kit (Millipore, Billerica, MA, USA) was used in this study. Briefly, 1×10^5 endothelial cells in 250 μl endothelial cell culture medium were loaded into each insert. After cells grew to >95% confluence, endothelial cell monolayers were activated with 20 ng ml^{-1} of recombinant human TNF-α for 4 h. Tumour cells (1×10^5) were suspended in 250 μl serum-free media and loaded into the insert. Tumour cells were allowed to migrate for 24 h at 37 °C. Cells that migrated to the bottom of the inserts were fixed with 100% methanol, stained with crystal violet and counted on a microscope.

Preparation of E-selectin-functionalized microtube and rolling experiments. Fifty centimetre-long microrenathane microtubes with 300 μm inner diameter (Braintree Scientific, Braintree, MA, USA) were first washed with 1× PBS and then coated with 10 μg ml^{-1} of recombinant protein G (Calbiochem, Frankfurt, Germany) for 1 h at room temperature. Microtubes were incubated with 0.125 μg ml^{-1} of recombinant mouse E-selectin/Fc chimera for 2 h. The surface was then blocked with 5% fat-free milk for 0.5 h to avoid non-specific interaction of cells with the tube surface. Tubes were washed with PBS^{++} (PBS saturated with calcium chloride; Invitrogen) and dissociated monolayer cells at a concentration of 1×10^6 cells per ml in PBS^{++} were perfused through at 2 dyn cm^{-2} using a syringe pump (IITC Life Sciences, Woodland Hills, CA, USA). Functionalized microtubes were

secured to the stage of an Olympus IX81 motorised inverted microscope (Olympus America, Melville, NY, USA). A CCD camera (Hitachi, Tokyo, Japan) and DVD recorder (Sony Electronics, Tokyo, Japan) were used to record experiments. Videos were later analysed using in-house ImageJ (NIH, Bethesda, MA, USA) stack tools to quantify rolling velocities. The number of cells per frame of rolling video was manually counted.

Animal studies. All mice were handled according to the Guide for the Care and Use of Laboratory Animals in compliance with UK-based guidelines. All experimental procedures and protocols were approved by the Institutional Animal Care and Use Committee of Cornell University (Protocol number 2011-0051). Male C57BL/6 mice (age 6–8 weeks) were anaesthetised by 2.5% isoflurane on the day of injections. On day 0, anaesthetised animals were injected with 1×10^5 cells suspended in 100 μl sterile DPBS containing 300 μg/ml D-luciferin into the left ventricle of the heart by non-surgical means via a 29 G needle (BD Biosciences). After injection, mice were subject to bioluminescence imaging (BLI).

Bioluminescence imaging. Bioluminescence imaging was performed with a CCD camera mounted in a light-tight specimen box (Xenogen, Waltham, MA, USA). Imaging and quantification of signals were controlled by the acquisition and analysis software Living Image (Xenogen). Anaesthetised mice were placed in the IVIS Imaging System and imaged from ventral views $\sim$10–15 min after intraperitoneal injection of D-luciferin at 150 mg kg^{-1} body weight. For experiments on day 0, successful intracardiac injections were indicated by images showing systemic bioluminescence distributed throughout the animal. Only mice with evidence of a satisfactory injection continued in the experiments. Assessment of subsequent metastasis was monitored *in vivo* after 1 week.

Histology. Mouse hind legs were fixed in 4% formaldehyde in PBS overnight and then decalcified in 10% formic acid in 10% formalin/PBS overnight. Decalcified hind legs were embedded in paraffin after tissue processing (dehydration, clearance and impregnation). Serial sections (5 μm) from each tissue block were cut onto slides and every fifth section was stained with hematoxylin and eosin (H&E) as previously described (Granot *et al*, 2011). Hematoxylin and eosin-stained slides were imaged with an upright Olympus BX-50 microscope equipped with a Moticam 2300 colour camera (Cole-Parmer, Vernon Hills, IL, USA).

Statistical analysis. All statistical analyses were performed using GraphPad Prism 5.0a for Mac OS X (San Diego, CA, USA). One-way ANOVA followed by Tukey's post test was used to compare statistical significance in the characterisation of rolling velocity, number of rolling cells, TEM and quantification of bioluminescence signals. When analysing gene expression of FTs in the NCBI database, significance was calculated by Student's *t*-test.

RESULTS

Mouse PCa cells do not express ESLs. E-selectin is a transmembrane glycoprotein that binds ESLs through its extracellular domain in a Ca^{2+}-dependent manner (Graves *et al*, 1994). Three representative mouse PCa cell lines (TRAMP-C1, TRAMP-C2 and RM1) were examined in this study. TRAMP-C1 and TRAMP-C2 were derived from the TRAMP mouse (Foster *et al*, 1997). This model was generated by overexpressing SV40, which suppresses p53 and Rb to mimic loss of function in tumour suppressor genes. In contrast, the RM1 cell line was developed from the mouse prostate reconstitution model (Thompson *et al*, 1989). This model overexpresses the oncogene Ras. To test their binding to mouse E-selectin, cells were incubated with dimerised E-selectin-human IgG Fc chimera and fluorescently labelled anti-human Fc. This measurement showed that all three cell lines express low level of ESLs (Figure 1A).

Mouse PCa cells express certain glycoprotein ESLs but not sLe^x. The glycoproteins PSGL-1 and CD44 have been identified as ESLs in human PCa, colon cancer and breast cancer (Dimitroff *et al*, 2005; Burdick *et al*, 2006; Zen *et al*, 2008). It is not clear whether the lack of functional ESLs is because of the absence of similar glycoproteins or a lack of sLe^x in mouse PCa cells (Figure 1B). Antibodies recognising mouse PSGL-1 and CD44 were applied to TRAMP-C1, TRAMP-C2 and RM1 cells. None of them were found to express PSGL-1; however, CD44 is present on the cell surface of all three cell lines (Figure 1C). These glycoproteins serve as scaffolds to present the tetrasaccharide sLe^x, which can directly interact with E-selectin. Using an antibody that recognises sLe^x (HECA-452), it was found that none of these mouse PCa cell

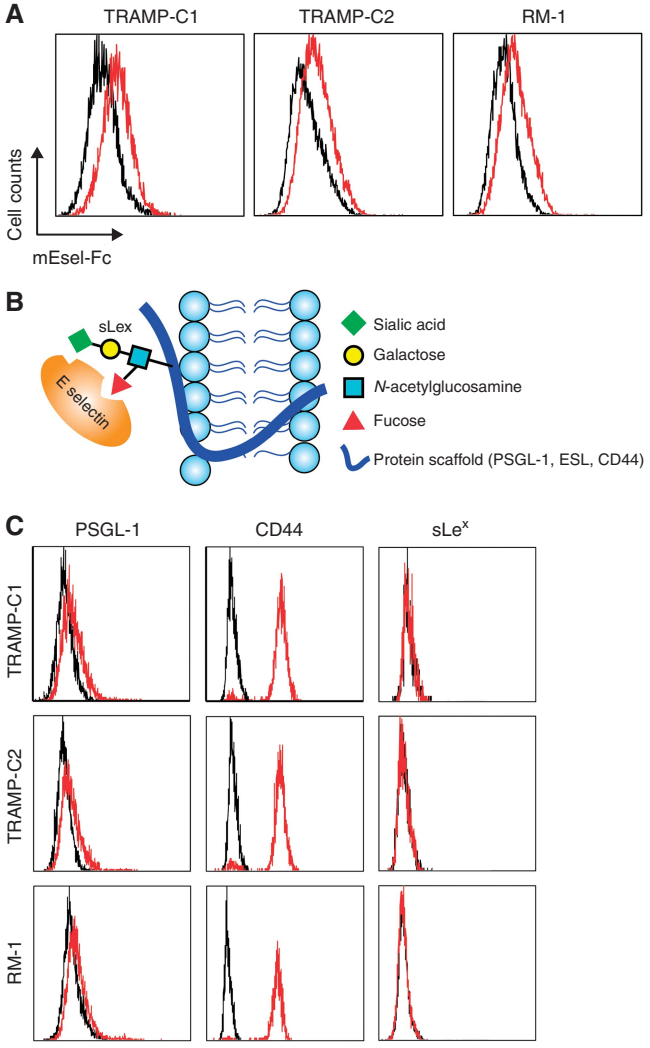

Figure 1. Characterisation of ESLs in mouse PCa cells. (**A**) Mouse PCa cells have low binding affinity to E-selectin. TRAMP-C1, TRAMP-C2 and RM1 were assayed for mouse E-selectin-Fc chimera binding. Staining was performed in the presence of 2 mM Ca^{2+} (red histograms) or 1 mM EDTA (black histograms); $n=3$. Representative histograms from three experiments are shown. (**B**) A cartoon showing components of ESLs required for the binding of ESLs to E-selectin. (**C**) Mouse PCa cells express ESL scaffold but lack essential carbohydrate. Mouse PSGL-1, CD44 and sLe^x were assayed with PE-anti-PSGL-1, FITC-anti-CD44 and FITC-HECA-452 antibodies (red histograms) or corresponding isotypes (black histograms); $n=3$. Representative histograms from three experiments are shown.

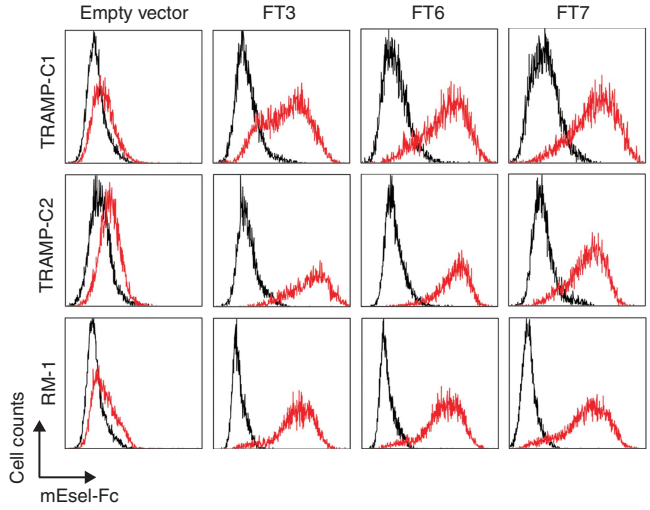

Figure 2. α-1,3-Fucosyltransferases are potent inducers of E-selectin binding in mouse PCa cells. Retrovirus packaged with empty vector (vehicle control), FT3, FT6 and FT7 were transduced into TRAMP-C1, TRAMP-C2 and RM1 cells. Stable cells were established under selection with G418 (400 $\mu g\,ml^{-1}$) for 2 weeks. Afterwards, cells were assayed for mouse E-selectin-Fc chimera binding. Staining in the presence of 2 mM Ca^{2+} (red histograms) or 1 mM EDTA (black histograms); $n=2$. Representative histograms from two experiments are shown.

lines express sLe^x (Figure 1C). Although previous work suggests that mouse ESLs are not recognised by the HECA-452 antibody because of differences in sialic-acid composition compared with human ESLs (Mitoma *et al*, 2009), it was found in the present study that the introduction of fucose by overexpression of α-1,3 FTs restored the binding of HECA-452 to mouse cell lines. This validates the use of HECA-452 to identify sLe^x in this work (Supplementary Figure 1). Thus, we may conclude that the lack of sLe^x is likely responsible for the deficiency in E-selectin binding.

FT3, FT6 and FT7 induce functional ESL expression on mouse PCa cells. The final step of sLe^x synthesis on glycoproteins involves the transfer of fucose to *N*-acetylglucosamine catalysed by α-1,3-FT. The upregulation of α-1,3 FT3, 6 and 7 in human metastatic PCa tissues motivates the examination of whether FT3, FT6, or FT7 could be involved directly in the expression of sLe^x in mouse PCa cell lines (Barthel *et al*, 2008, 2009). cDNA-encoding human FT3, FT6 and FT7 were packaged into retroviral particles and transduced into the TRAMP-C1, TRAMP-C2 and RM1 cell lines to establish stable cell clones. Indeed, overexpression of FT3, FT6 or FT7 restored E-selectin-binding in mouse PCa cells compared with empty vector-transduced cell lines (Figure 2). Thus, overexpression of FTs completes the final step of sLe^x synthesis and enables E-selectin binding in mouse PCa cells.

Characterisation of rolling behaviour of FT-transduced cells. We next examined E-selectin binding in a dynamic fluid flow system. A previously established flow-based microtube system was employed to mimic the bone microvascular environment

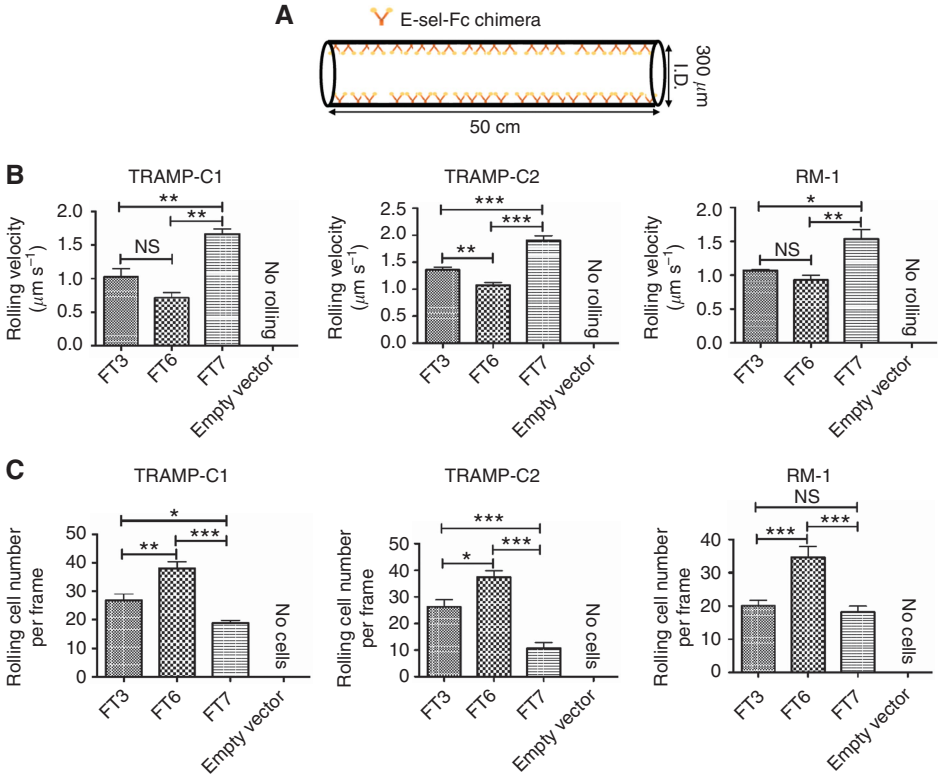

Figure 3. α-1,3-Fucosyltransferases mediate robust but distinct mouse PCa cell rolling in E-selectin-coated microtubes. (**A**) A cartoon of a biomimetic microtube is shown. The inner surface of microtubes were functionalized with protein G and E-selectin-Fc chimera to mimic constitutive E-selectin expression on BM endothelial cells. (**B**) Cell-rolling velocity for α-1,3-FT-transduced TRAMP-C1, TRAMP-C2 and RM1, respectively. Thirty rolling cells were recorded under physiological WSS of 2 dyn cm^{-2} from each independent experiment. 'No rolling' indicates that empty vector-transfected cells failed to roll on E-selectin surfaces. Results are the mean ± s.e.m. of three experiments; $^{**}P<0.01$, $^{***}P<0.001$. (**C**) Number of rolling cells interacting with E-selectin-functionalized surfaces per frame under physiological WSS of 2 dyn cm^{-2}. Ten frames were recorded for each experiment. Results are the mean ± s.e.m. of three experiments; $^{**}P<0.01$, $^{***}P<0.001$.

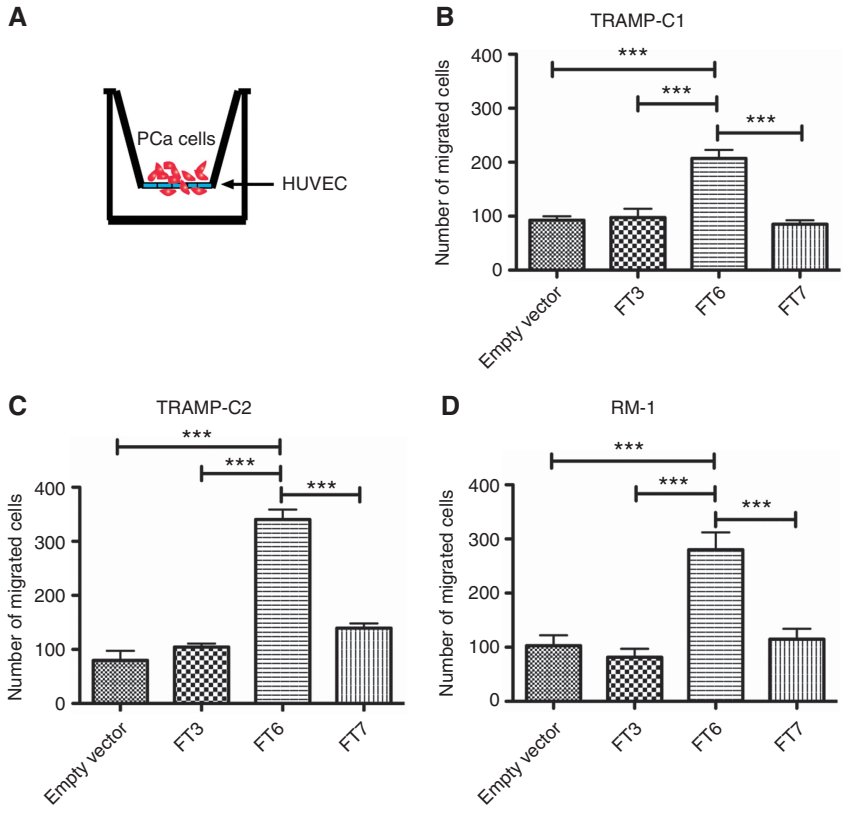

Figure 4. α-1, 3 FTs induce differential TEM. (**A**) A cartoon depicting the TEM assay is shown. Nearly confluent HUVEC monolayers were stimulated with TNF-α for 4 h before PCa cells were seeded. (**B–D**) Number of cells that migrated through a monolayer of HUVEC after incubation for 24 h. Results are the mean ± s.e.m. of three experiments; ***$P<0.001$.

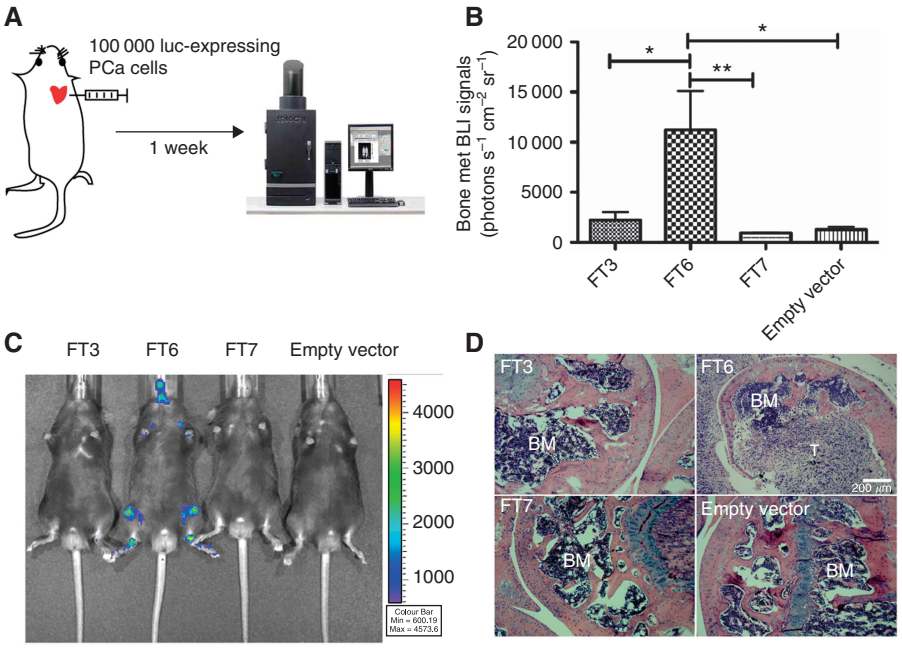

Figure 5. FT6 induces the highest incidence of bone metastasis using TRAMP-C2 cells in C57BL/6 mice. (**A**) A cartoon illustrating the procedures including intracardiac injection and BLI is shown. (**B**) Quantification of bone metastases in femurs and tibias 1 week after inoculation of PCa cells. BLI signals collected on day 7 were normalised to whole-body BLI on day 0. FT6-induced statistically significant bone metastasis compared with empty vector, FT3 and FT7 groups. For each group, $n=6$. The experiment was repeated twice; results are mean ± s.e.m. from two independent experiments; *$P<0.05$, **$P<0.01$. (**C**) Representative BLI images taken 1 week after PCa inoculation. Heat bar is represented as counts. Bioluminescence imaging signals < 600 counts were considered noise and removed per manufacturer's suggestion. (**D**) Representative images of H&E staining from BLI-positive areas. Bioluminescence imaging was found to come largely from femurs proximal to knee joints. Abbreviations: BM = bone marrow, T = tumour.

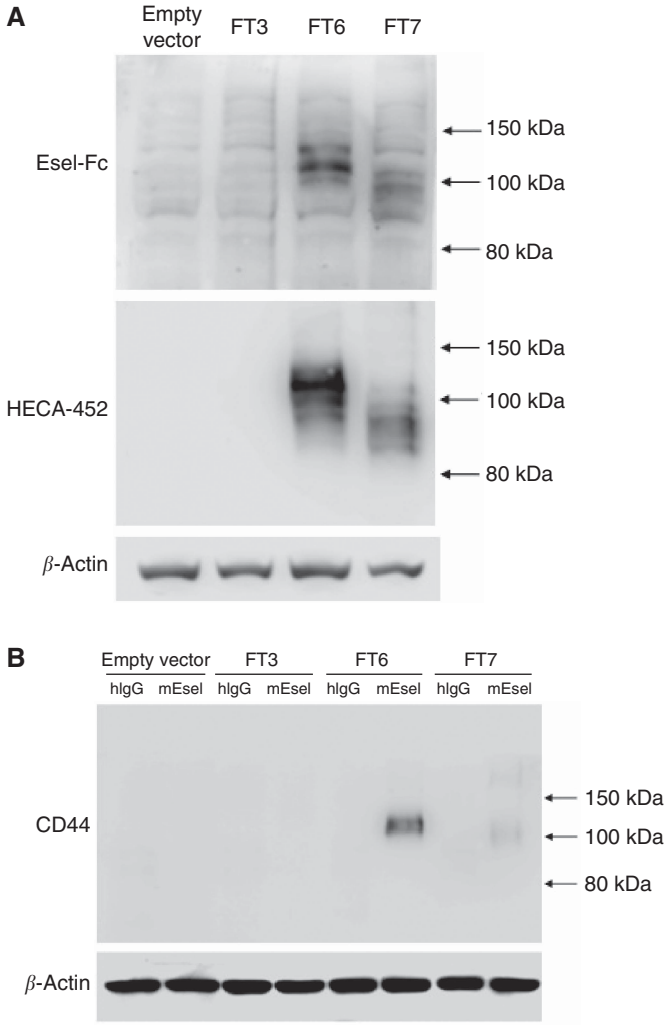

Figure 6. CD44 is a primary ESL following FT6 overexpression. (**A**) Western blotting of membrane proteins from FT3-, FT6- and FT7-transduced TRAMP-C2 cells. Distinct patterns were identified after proteins were probed with E-selectin-Fc and anti-sLe^x mAb HECA-452. Empty vector-transduced TRAMP-C2 served as a background control. Anti-β actin was used as a loading control. (**B**) E-selectin-Fc immunoprecipitates from FTs-transduced TRAMP-C2 proteins were subjected to western blotting and immunostained with anti-CD44. Human IgG immunoprecipitates were not reactive with anti-CD44 indicating specific interaction between E-selectin and CD44. Only FT6 cells generated a CD44-reactive band showing that FT3 and FT7 were unable to modify CD44 to become a functional ESL.

(Narasipura and King, 2009; Rana *et al*, 2009, 2012; Hsu *et al*, 2011. Briefly, the inner surface of microtubes were coated with mouse E-selectin-Fc chimera (Figure 3A). To simulate circulating behaviour, PCa cells were perfused at physiological wall shear stress (WSS) through the microtube lumen, and their rolling behaviour was characterised by measuring the rolling velocity and recording the number of interacting cells. In all three cell lines, FT6-transduced cells exhibited the slowest rolling velocity under physiological WSS of 2 dyn cm^{-2} (Figure 3B). The rolling adhesion was Ca^{2+} dependent, as flushing with 1 mM EDTA abolished cell binding as expected for E-selectin adhesion (data not shown). In contrast, cells transduced with empty vector were unable to roll or interact with E-selectin-coated microtubes (Figure 3B). In addition, FT6-overexpressing cells displayed the highest number of rolling cells interacting with E-selectin-coated surfaces (Figure 3C, Supplementary Figure 2). The behaviour in this biomimetic *in vitro* system suggests that ESLs may support the recruitment of CTCs from circulation to the bone endothelium *in vivo*.

TEM of FT-transduced cells. After CTCs roll and form firm adhesions with the endothelial layer in BM microvessels, CTCs must breach this layer to establish micrometastases, a process referred to as TEM. To assess TEM capability, empty vector or FT-transduced TRAMP-C1, TRAMP-C2 and RM1 cells were seeded on confluent monolayers of endothelial cells pre-stimulated with TNF-α to transiently express E-selectin. The potential of TEM was measured by counting cells that migrated through the layer after 24 h incubation (Figure 4A). Notably, FT6-transduced cells showed greater TEM ability than empty vector, FT3- and FT7-transduced cells (Figures 4B–D, Supplementary Figure 3).

FT6 promotes the greatest potential for BM metastasis. We next investigated whether the differential rolling velocity and TEM are sufficient to lead to distinct BM metastases in immune-competent mice. Equal numbers of empty vector or FT-transduced TRAMP-C2 cells stably expressing firefly luciferase were injected into the left ventricle of C57BL/6 mice. The intracardiac route was selected to allow for systemic dissemination of CTCs before becoming entrapped in the microvessels of the lung (Campbell *et al*, 2012; Zou *et al*, 2013). One week after cell injection, bone metastases were quantified by measuring luminescence signal in the tibia and femur (Figure 5A). The bioluminescence signal from the tibias and femurs were normalised to whole-body luminescence signal taken on day 0. Consistent with the *in vitro* findings, FT6-transduced TRAMP-C2 cells developed the highest metastatic burden in the bone (Figures 5B and C). Further examination of BM invasion by H&E staining revealed that only FT6-transduced TRAMP-C2 cells established significant metastases in the femur proximal to the knee joint (Figure 5D).

FT6 converts CD44 to a functional ESL. To identify candidate ESLs induced by the overexpression of FTs, the glycoproteins from total lysates of FT-transduced TRAMP-C2 cells were examined by western blotting. Both mouse E-selectin-Fc and HECA-452 identified protein bands of a similar size, indicating that the ESLs formed after overexpression of FTs are positive for sLe^x- or sLe^x-like glycan (Figure 6A). Whereas FT3-transduced cells were not detectable by either E-selectin-Fc or HECA-452, FT6 and FT7 generated unique patterns of ESLs in the blots. It is possible that FT3-induced ESLs are primarily glycolipids or glycoproteins that cannot be readily detected because of the denaturation step of western blotting. Noting that the slowest rolling velocity and greatest TEM found *in vitro* as well as the highest incidence of bone metastasis *in vivo* was observed for FT6, the identity of unique glycoproteins was further investigated in FT6-transduced TRAMP-C2. The distinct fragment produced by FT6 lysate was excised from SDS–PAGE gel after superimposition to the band of a similar size in blots and analysed by mass spectrometry. An E-selectin-binding, sLe^x-bearing protein, CD44, was identified and further validated through immunoprecipitation by beads conjugated to E-selectin-Fc (Figure 6B). Consistent with human studies, CD44 has been found to be a key protein that is involved in the adherence of metastatic prostate and breast cancer cells to BM endothelial cells (Draffin *et al*, 2004).

FT6 expression correlates with clinical PCa progression. To access the clinical relevance of FT6 in human PCa, the gene expression profile of FT6 was analysed through public microarray repositories from the NCBI Gene Expression Omnibus (profile number GDS2545, Metastatic PCa HG-U95A). It consists of three categories: (1) normal prostate tissue adjacent to PCa tumour ($n=63$), (2) primary PCa tumours ($n=65$) and (3) distant metastasis samples ($n=25$). We found higher levels of FT6 in

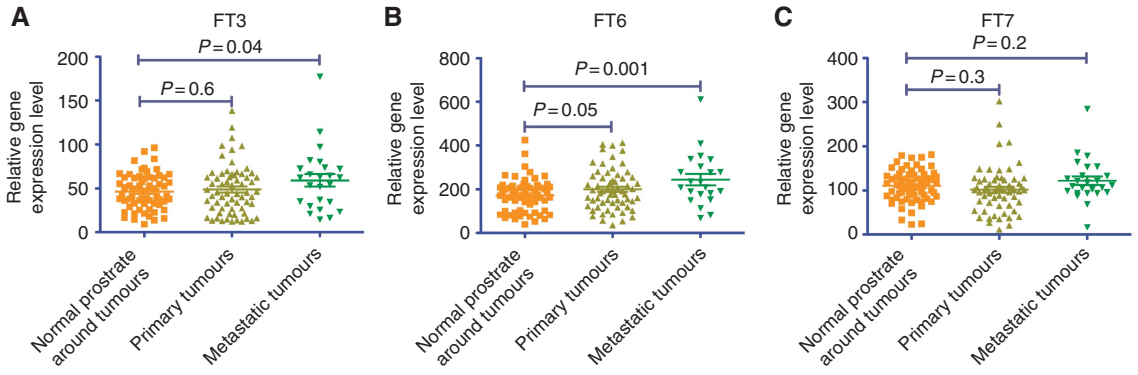

Figure 7. Gene expression analysis of FTs in clinical PCa. The NCBI Gene Expression Omnibus (GEO) data set GDS2545 was utilised for profiling the expression of (**A**) FT3, (**B**) FT6 and (**C**) FT7 in (1) normal prostate tissue adjacent to tumour ($n=63$), (2) primary tumours ($n=65$) and (3) metastatic prostate tumour samples ($n=25$), and significance was analysed by Student's *t*-test.

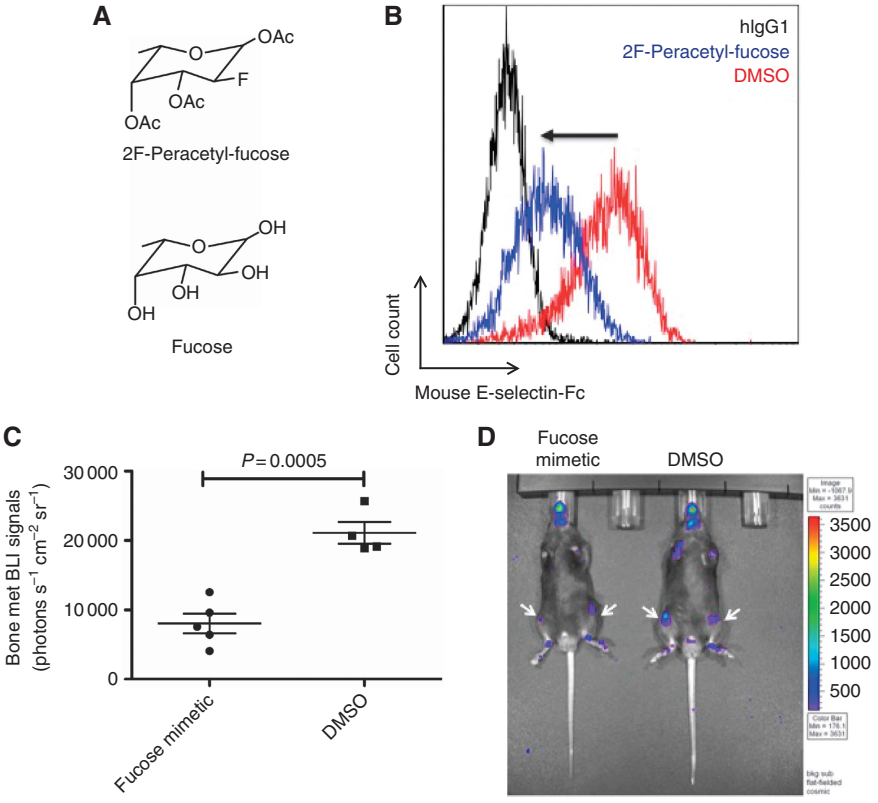

Figure 8. Inhibition of FT6 by fucose mimetic (2F-peracetyl-fucose) reduces bone metastasis. (**A**) Molecular structure of 2F-peracetyl-fucose and natural fucose. (**B**) Fucosyltransferase 6-transduced TRAMP-C2 cells were treated with 20 μg ml^{-1} 2F-peracetyl-fucose or 0.2% DMSO for 96 h. The expression of ESLs was detected by human IgG isotype or mouse E-selectin-Fc at 10 μg ml^{-1}. (**C**) Pretreatment with 2F-peracetyl-fucose reduced bone metastasis *in vivo*. Fucosyltransferase 6-transduced TRAMP-C2 cells with the same treatment as (**B**) were injected into the left ventricle of C57BL/6 mice. Bone metastases in femurs and tibias were quantified by BLI 1 week later. Significance was analysed by Student's *t*-test. DMSO group, $n=5$. 2F-peracetyl-fucose group, $n=4$. (**D**) Representative image of bone metastases in study (**C**). Arrows indicate areas of bone metastases.

primary prostate tumours ($P=0.05$) and metastatic tumours ($P=0.001$) in comparison with normal prostate epithelium adjacent to primary PCa tumours (Figure 7B, Supplementary Table). No significant difference was found when examining FT3 and FT7 in the same tissues, except for an increase in FT3 expression in distant metastasis samples compared with normal prostate epithelium adjacent to tumours ($P=0.04$; Figure 7A and C, Supplementary Table).

α-1, 3-FT inhibitor reduces FT6-dependent bone metastasis. The *in vivo* experiments in this work along with gene expression profiles from clinical samples support the idea that FT6 may be one of the key mediators that drives bone metastasis. Thus, it is of therapeutic interest to explore whether the inhibition of FT6 can reduce bone metastasis in our mouse model. To this end, fluorinated fucose mimetic (2F-peracetyl-fucose) was utilised to inhibit the activity of FT6 (Figure 8A). Following 3 days of incubation with 20 μg ml^{-1} 2F-peracetyl-fucose, FT6-transduced TRAMP-C2 showed reduced E-selectin binding (Figure 8B). This concentration did not compromise cell viability (data not shown), consistent with a prior study in which a three-fold higher concentration did not affect the viability of leukocytes

(Rillahan *et al*, 2012). To assay the efficacy of this fucose mimetic *in vivo*, FT6-transduced TRAMP-C2 cells that received the same treatment or vesicle control (DMSO) were injected into C57BL/6 mice via the left ventricle. One week later, fucose mimetic-treated cells produced significantly fewer and smaller bone metastases compared with DMSO treatment quantified by BLI (Figure 8C and D). As 2F-peracetyl-fucose is highly cell permeable and has not been shown to reduce cell viability in prior studies, we reason that it represents a potential therapeutic for the reduction of bone metastasis.

DISCUSSION

In this work, we aimed to dissect the molecular mechanism of why bone metastasis is a frequent occurrence in the human disease but rare in mouse. Our results indicated that the lack of functional ESLs in mouse cell lines may partly explain this discrepancy. As ESLs are composed of a scaffold protein or lipid decorated by the tetrasaccride sLe^x, we further identified a lack of sLe^x in mouse PCa cells. However, overexpression of human α-1,3 FTs in mouse PCa cells restored E-selectin binding and led to the rolling of PCa cells in E-selectin-coated microtubes under physiological flow conditions. Interestingly, the different FTs (FT3, FT6 and FT7) showed differential rolling velocities and TEM capability *in vitro*. Among the three mouse PCa cell lines tested (TRAMP-C1, TRAMP-C2 and RM1), FT6-transduced cells showed the slowest rolling velocity and the highest degree of TEM. To correlate these *in vitro* findings with *in vivo* metastatic potential, we inoculated FT-transduced TRAMP-C2 cells labelled with firefly luciferase into the left ventricle of wild-type C57BL/6 mice. Within 1 week, the FT6-overexpressing cells promoted significant bone metastasis in the tibia and femur as detected by BLI. We further identified CD44 as a primary ESL in cells expressing FT6 but not FT3 or FT7. This correlates with previous studies in human cells where CD44 promoted the adherence of metastatic cancer cells and mesenchymal stem cells to BM endothelial cells (Draffin *et al*, 2004; Burdick *et al*, 2006; Sackstein *et al*, 2007; Zen *et al*, 2008; Sackstein, 2012).

Interestingly, previous work by the Dimitroff lab showed that FT7 rather than FT3 or FT6 promoted trafficking of human PC3 PCa cells to immunodeficient mouse BM (Barthel *et al*, 2009). This may reflect inherent species-dependent differences between mouse and human-derived PCa cells. It should be noted that the mouse genome does not include the FT3 or FT6 genes and only FT4 and FT7 are inherently present to support E-selectin-mediated leukocyte rolling (Weninger *et al*, 2000; Homeister *et al*, 2001). Expression of human FT6 in mouse PCa cells may compensate for this loss during evolution. Despite such interspecies differences, FT6 has been found to be elevated in other human bone metastatic PCa and breast cancer cell lines (Matsuura *et al*, 1998; Barthel *et al*, 2008). Moreover, one of significant findings in this work is that FT6 gene expression correlates best to clinical PCa progression and metastasis as revealed by public microarray repositories from the NCBI Gene Expression Omnibus.

Previous study in breast cancer indicates that ESLs mediate breast cancer cell TEM and that E-selectin-blocking antibody can functionally abolish this migration *in vitro* (Zen *et al*, 2008). Although it is not clear whether FT has a role in the TEM of breast cancer cells, it was shown that ESLs prime TEM of human mesenchymal stromal cells (MSCs) and direct them to bone by maintaining ESL expression in MSCs via FT6 (Sackstein et al, 2007, 2008; Thankamony and Sackstein, 2011). Viewing this previous work in light of the current study, we speculate that therapeutic targeting of ESLs could prevent both E-selectin-mediated trafficking to bone and TEM in the reduction of PCa bone metastasis.

Many cancers have been found to associate with inflammation as exemplified by the infiltration of tumour-associated macrophages and regulator T cells, and inflammation can further aggravate cancer progression (Grivennikov *et al*, 2010). In this study, we utilised the fucose mimetic 2F-peracetyl-fucose to inhibit FT enzyme activity and achieved a significant reduction of bone metastasis in the FT6-induced bone metastasis mouse model. This inhibitor along with other sugar mimetics have been suggested to suppress inflammation by inhibiting the synthesis of ESLs in infiltrating leukocytes without affecting cell viability (Barthel *et al*, 2011; Rillahan *et al*, 2012). We suggest that fucose mimetics may be potential drugs that target the vicious cycle of inflammation and cancer progression. In addition to these sugar inhibitors, siRNA that targets specific FTs can also be utilised (Yin *et al*, 2010).

This newly developed experimental metastasis model has several advantages over existing mouse models of bone metastasis: (1) It bypasses complicated surgical implantation of PCa cells in the bone. Moreover, the direct intraosseous implantation bypasses several crucial steps in the metastatic cascade: survival in the bloodstream, rolling and extravasation (McCabe *et al*, 2008); (2) Is less time consuming than iterative selection of the bone metastatic PCa cells (Power *et al*, 2009); (3) the use of wild-type mouse allows for the study of PCa development in an immunocompetent background, which considers the involvement of the immune system.

ACKNOWLEDGEMENTS

We thank Johanna M Dela Cruz for providing technical imaging support at the Cornell Microscopy and Imaging Facility (MIF) and Dr Sheng Zhang at the Cornell Proteomics and Mass Spectrometry Core Facility for protein mass spectrometry. We thank Christine M Peterson and David E Mooneyhan for teaching intracardiac injection at the Cornell Center for Animal Resources and Education (CARE). This work was supported by NIH/NCI Grants (U54 CA143876, MRK; R01 CA173610, CJD), NIH/NCCAM Grant (R01AT004628, CJD), American Cancer Society Postdoctoral Fellowship (10-227, SRB), and NIH Kirschstein-NRSA Postdoctoral Fellowship (F32 CA144219-01A1, SRB).

CONFLICT OF INTEREST

The authors declare no conflicts of interest.

REFERENCES

Barthel SR, Antonopoulos A, Cedeno-Laurent F, Schaffer L, Hernandez G, Patil SA, North SJ, Dell A, Matta KL, Neelamegham S, Haslam SM, Dimitroff CJ (2011) Peracetylated 4-fluoro-glucosamine reduces the content and repertoire of N- and O-glycans without direct incorporation. *J Biol Chem* **286**(24): 21717–21731.

Barthel SR, Gavino JD, Wiese GK, Jaynes JM, Siddiqui J, Dimitroff CJ (2008) Analysis of glycosyltransferase expression in metastatic prostate cancer cells capable of rolling activity on microvascular endothelial (E)-selectin. *Glycobiology* **18**(10): 806–817.

Barthel SR, Hays DL, Yazawa EM, Opperman M, Walley KC, Nimrichter L, Burdick MM, Gillard BM, Moser MT, Pantel K, Foster BA, Pienta KJ, Dimitroff CJ (2013) Definition of molecular determinants of prostate cancer cell bone extravasation. *Cancer Res* **73**(2): 942–952.

Barthel SR, Wiese GK, Cho JH, Opperman MJ, Hays DL, Siddiqui J, Pienta KJ, Furie B, Dimitroff CJ (2009) Alpha 1,3 fucosyltransferases are master regulators of prostate cancer cell trafficking. *Proc Natl Acad Sci USA* **106**(46): 19491–19496.

Bu P, Chen KY, Chen JH, Wang L, Walters J, Shin YJ, Goerger JP, Sun J, Witherspoon M, Rakhilin N, Li J, Yang H, Milsom J, Lee S, Zipfel W,

Jin MM, Gumus ZH, Lipkin SM, Shen X (2013) A microRNA miR-34a-regulated bimodal switch targets notch in colon cancer stem cells. *Cell Stem Cell* **12**(5): 602–615.

Burdick MM, Chu JT, Godar S, Sackstein R (2006) HCELL is the major E- and L-selectin ligand expressed on LS174T colon carcinoma cells. *J Biol Chem* **281**(20): 13899–13905.

Campbell JP, Merkel AR, Masood-Campbell SK, Elefteriou F, Sterling JA (2012) Models of bone metastasis. *J Vis Exp* **67**: e4260.

de Vries T, Knegtel RMA, Holmes EH, Macher BA (2001) Fucosyltransferases: structure/function studies. *Glycobiology* **11**(10): 119R–128R.

Dimitroff CJ, Descheny L, Trujillo N, Kim R, Nguyen V, Huang W, Pienta KJ, Kutok JL, Rubin MA (2005) Identification of leukocyte E-selectin ligands, P-selectin glycoprotein ligand-1 and E-selectin ligand-1, on human metastatic prostate tumor cells. *Cancer Res* **65**(13): 5750–5760.

Dimitroff CJ, Lechpammer M, Long-Woodward D, Kutok JL (2004) Rolling of human bone-metastatic prostate tumor cells on human bone marrow endothelium under shear flow is mediated by E-selectin. *Cancer Res* **64**(15): 5261–5269.

Draffin JE, McFarlane S, Hill A, Johnston PG, Waugh DJJ (2004) CD44 potentiates the adherence of metastatic prostate and breast cancer cells to bone marrow endothelial cells. *Cancer Res* **64**(16): 5702–5711.

Foster BA, Gingrich JR, Kwon ED, Madias C, Greenberg NM (1997) Characterization of prostatic epithelial cell lines derived from transgenic adenocarcinoma of the mouse prostate (TRAMP) model. *Cancer Res* **57**(16): 3325–3330.

Gingrich JR, Barrios RJ, Morton RA, Boyce BF, DeMayo FJ, Finegold MJ, Angelopoulou R, Rosen JM, Greenberg NM (1996) Metastatic prostate cancer in a transgenic mouse. *Cancer Res* **56**(18): 4096–4102.

Granot Z, Henke E, Comen EA, King TA, Norton L, Benezra R (2011) Tumor entrained neutrophils inhibit seeding in the premetastatic lung. *Cancer Cell* **20**(3): 300–314.

Graves BJ, Crowther RL, Chandran C, Rumberger JM, Li S, Huang KS, Presky DH, Familletti PC, Wolitzky BA, Burns DK (1994) Insight into E-selectin ligand interaction from the crystal-structure and mutagenesis of the Lec Egf domains. *Nature* **367**(6463): 532–538.

Grivennikov SI, Greten FR, Karin M (2010) Immunity, inflammation, and cancer. *Cell* **140**(6): 883–899.

Homeister JW, Thall AD, Petryniak B, Maly P, Rogers CE, Smith PL, Kelly RJ, Gersten KM, Askari SW, Cheng G, Smithson G, Marks RM, Misra AK, Hindsgaul O, von Andrian UH, Lowe JB (2001) The alpha(1,3) fucosyltransferases FucT-IV and FucT-VII exert collaborative control over selectin-dependent leukocyte recruitment and lymphocyte homing. *Immunity* **15**(1): 115–126.

Hsu JW, Yasmin-Karim S, King MR, Wojciechowski JC, Mickelsen D, Blair ML, Ting HJ, Ma WL, Lee YF (2011) Suppression of prostate cancer cell rolling and adhesion to endothelium by 1 alpha,25-dihydroxyvitamin D-3. *Am J Pathol* **178**(2): 872–880.

Li J, King MR (2012) Adhesion receptors as therapeutic targets for circulating tumor cells. *Front Oncol* **2**(79): 1–9.

Matsumoto M, Atarashi K, Umemoto E, Furukawa Y, Shigeta A, Miyasaka M, Hirata T (2005) CD43 functions as a ligand for E-selectin on activated T cells. *J Immunol* **175**(12): 8042–8050.

Matsuura N, Narita T, Hiraiwa N, Hiraiwa M, Murai H, Iwase Y, Funahashi H, Imai T, Takagi H, Kannagi R (1998) Gene expression of fucosyl- and sialyl-transferases which synthesize sialyl Lewis(x), the carbohydrate ligands for E-selectin, in human breast cancer. *Int J Oncol* **12**(5): 1157–1164.

McCabe NP, Madajka M, Vasanji A, Byzova TV (2008) Intraosseous injection of RM1 murine prostate cancer cells promotes rapid osteolysis and periosteal bone deposition. *Clin Exp Metastasis* **25**(5): 581–590.

Mitoma J, Miyazaki T, Sutton-Smith M, Suzuki M, Saito H, Yeh JC, Kawano T, Hindsgaul O, Seeberger PH, Panico M, Haslam SM, Morris HR, Cummings RD, Dell A, Fukuda M (2009) The N-glycolyl form of mouse sialyl Lewis X is recognized by selectins but not by HECA-452 and FH6 antibodies that were raised against human cells. *Glycoconjugate J* **26**(5): 511–523.

Narasipura SD, King MR (2009) P-selectin-coated microtube for the purification of CD45 + hematopoietic cells directly from human peripheral blood. *Blood Cell Mol Dis* **42**(2): 136–139.

Power CA, Pwint H, Chan J, Cho J, Yu Y, Walsh W, Russell PJ (2009) A novel model of bone-metastatic prostate cancer in immunocompetent mice. *Prostate* **69**(15): 1613–1623.

Rana K, Liesveld JL, King MR (2009) Delivery of apoptotic signal to rolling cancer cells: a novel biomimetic technique using immobilized TRAIL and E-selectin. *Biotechnol Bioeng* **102**(6): 1692–1702.

Rana K, Reinhart-King CA, King MR (2012) Inducing apoptosis in rolling cancer cells: a combined therapy with aspirin and immobilized TRAIL and E-selectin. *Mol Pharmaceut* **9**(8): 2219–2227.

Rillahan CD, Antonopoulos A, Lefort CT, Sonon R, Azadi P, Ley K, Dell A, Haslam SM, Paulson JC (2012) Global metabolic inhibitors of sialyl- and fucosyltransferases remodel the glycome. *Nat Chem Biol* **8**(7): 661–668.

Saad F, Clarke N, Colombel M (2006) Natural history and treatment of bone complications in prostate cancer. *Eur Urol* **49**(3): 429–440.

Sackstein R (2012) Glycoengineering of HCELL, the human bone marrow homing receptor: sweetly programming cell migration. *Ann Biomed Eng* **40**(4): 766–776.

Sackstein R, Merzaban JS, Cain DW, Dagia NM, Spencer JA, Lin CP, Wohlgemuth R (2007) Ex vivo glycan engineering of membrane CD44 to create HCELL programs human mesenchymal stem cell trafficking to bone. *Blood* **110**(11): 72A.

Sackstein R, Merzaban JS, Cain DW, Dagia NM, Spencer JA, Lin CP, Wohlgemuth R (2008) Ex vivo glycan engineering of CD44 programs human multipotent mesenchymal stromal cell trafficking to bone. *Nat Med* **14**(2): 181–187.

Siegel R, Naishadham D, Jemal A (2012) Cancer Statistics, 2012. *CA Cancer J Clin* **62**(1): 10–29.

Sturge J, Caley MP, Waxman J (2011) Bone metastasis in prostate cancer: emerging therapeutic strategies. *Nat Rev Clin Oncol* **8**(6): 357–368.

Thankamony SP, Sackstein R (2011) Enforced hematopoietic cell E- and L-selectin ligand (HCELL) expression primes transendothelial migration of human mesenchymal stem cells. *Proc Natl Acad Sci USA* **108**(6): 2258–2263.

Thompson TC, Southgate J, Kitchener G, Land H (1989) Multistage carcinogenesis induced by ras and myc oncogenes in a reconstituted organ. *Cell* **56**(6): 917–930.

Weninger W, Ulfman LH, Cheng G, Souchkova N, Quackenbush EJ, Lowe JB, von Andrian UH (2000) Specialized contributions by alpha(1,3)-fucosyltransferase-IV and FucT-VII during leukocyte rolling in dermal microvessels. *Immunity* **12**(6): 665–676.

Wilt TJ, Ahmed HU (2013) Prostate cancer screening and the management of clinically localized disease. *Br Med J* **346**(1): 325–334.

Winkler IG, Barbier V, Nowlan B, Jacobsen RN, Forristal CE, Patton JT, Magnani JL, Levesque JP (2012) Vascular niche E-selectin regulates hematopoietic stem cell dormancy, self renewal and chemoresistance. *Nat Med* **18**(11): 1651–1657.

Yin XY, Rana K, Ponmudi V, King MR (2010) Knockdown of fucosyltransferase III disrupts the adhesion of circulating cancer cells to E-selectin without affecting hematopoietic cell adhesion. *Carbohyd Res* **345**(16): 2334–2342.

Zen K, Liu DQ, Guo YL, Wang C, Shan J, Fang M, Zhang CY, Liu Y (2008) CD44v4 is a major E-selectin ligand that mediates breast cancer cell transendothelial migration. *PLoS One* **3**: 3 e1826.

Zou M, Jiao J, Zou Q, Xu Y, Cheng M, Xu J, Zhang Y (2013) Multiple metastases in a novel LNCaP model of human prostate cancer. *Oncol Rep* **30**(2): 615–622.

Supplementary Information accompanies this paper on British Journal of Cancer website (http://www.nature.com/bjc)